Research Article

Performance of Sweet Potato's Leaf-Derived Activated Carbon for Hydrogen Sulphide Removal from Biogas

Geni Juma [iD], Revocatus Machunda, and Tatiana Pogrebnaya

Department of Materials, Energy Science and Engineering, The Nelson Mandela African Institution of Science and Technology, Arusha, Tanzania

Correspondence should be addressed to Geni Juma; genijm8@gmail.com

In this study, sweet potato leaf activated carbon (SpLAC) was prepared by the chemical activation method using KOH and applied as an adsorbent for H_2S removal from biogas. The study focused on the understanding of the effect of carbonization temperature (T_c), varying KOH : C activation ratio, flow rate (FR) of biogas, and mass of SpLAC on sample adsorption capacity. The BET analysis was performed for both fresh and spent activated carbons as well as for carbonized samples, which were not activated; also, the activated carbon was characterized by XRF and CHNS techniques. The results showed that removal efficiency (RE) of the SpLAC increased with increase carbonization temperature from 600 to 800°C and the mass of sorbent from 0.4 g to 1.0 g. The optimal test conditions were determined: 1.0 g of sorbent with a KOH : C ratio of 1 : 1, $T_c = 800$°C, and FR = 0.02 m³/h which resulted in a sorption capacity of about 3.7 g S/100 g of the SpLAC. Our findings corroborated that H_2S removal was contributed not only by the adsorption process with the pore available but also by the presence of iron in the sample that reacted with H_2S. Therefore, upon successful H_2S sorption, SpLAC is suggested as a viable adsorbent for H_2S removal from biogas.

1. Introduction

The world is striving to shift from the use of fossil fuel to renewable energy [1, 2]. Anaerobic microbial decomposition of organic substances produces not only the chief component methane (CH_4) but also undesirable impurities including hydrogen sulphide, carbon dioxide, and ammonia to mention but a few [3]. The resulting gas mixture, commonly known as biogas, is one of the best alternative energy sources; unlike fossil fuels, biogas is renewable, and its production does not cause environmental degradation.

Hydrogen sulphide contained in biogas gives rise to a variety of problems, including health problems to human beings. It affects several systems in the human body, and it causes serious environmental concerns due to its corrosiveness [4]. Following the importance of biogas as a replacement to fossil fuels, it is essential to remove H_2S from biogas before use [5].

Researchers have been reporting several methods for hydrogen sulphide from the biogas stream. These methods include chemical [6, 7], biological [8–10], and physical

methods [4, 11]. However, these technologies require high operational costs and technical complications, limiting their application at the household level and user on a small scale.

The adsorption has been a promising technique for H_2S removal from biogas [12]. To be able to circumvent the challenge of being too costly, particularly to low-income settings, researchers are focusing on searching for cheap adsorbents which are naturally available materials (wood, peat, coal, lignite, etc.) and agricultural, domestic, or industrial wastes or other products, for instance, red mud [13]. Several adsorbents derived from biomass waste have been reported for various applications. Water hyacinth-derived activated carbon using alkali activation at different carbonization temperatures was reported as potential adsorbent for biogas purification [4]. Activated carbon derived from chicken feathers [14] and made from jackfruit peels [15] was reported as a potential electrode material for removal of heavy metals from waste water by capacitive deionization technique. The ideal material precursor and the whole production chain of the adsorbent should be environmentally friendly. In recent studies, several adsorbents have been prepared and tested

for H$_2$S removal. Maize cob waste physically activated was found to have promising results in H$_2$S removal from biogas [16]. Also, H$_2$S adsorption by carbon impregnated with oxidants was performed in [17] whereby the reaction conditions are very important for better sorption capacity. Biochar derived from leaf waste was tested for adsorption of hydrogen sulphide [18] whereby 84.2% H$_2$S was effectively removed from biogas at a carbonization temperature of 400°C. Activated carbon from water hyacinths achieved up to 93% hydrogen sulphide removal efficiency in [4]. However, each adsorbent has its drawbacks; for instance, the use of water hyacinth has the potential of promoting its cultivation, which may lead to invading and dominating more water bodies. Oldoinyo Lengai volcanic ashes have been reported to have a hydrogen sulphide removal capacity of up to 1.00 g of sulphur/100 g of sorbent [19]; however, the exploitation of Oldoinyo Lengai volcanic ashes will lead to the destruction of the Oldoinyo Lengai conservation area. Zeolite is another efficient hydrogen removing material [20]. However, its utilization causes environmental degradation and is not locally available. The weaknesses of various materials in biogas purification call for continued efforts to search for better materials.

Sweet potatoes have been reported to have iron content, especially in the leaves [21, 22]. The plants grow fast and are abundantly available. The leaves can act as precursor materials for porous activated carbon [23]. In that study, sweet potato stalks and leaves were used to make AC in preparation of supercapacitor material with high performance in electrolytes. To add on that, the leaves can act as precursors of iron (iii) oxide that has been reported to have a removal capacity of a maximum 0.60 g H$_2$S/g Fe$_2$O$_3$ [24]. The fact that sweet potato plants grow fast and contain iron, that could facilitate H$_2$S removal, motivated choice of the plant. It is anticipated that due to the iron content, this material will be superior in hydrogen sulphide removal from biogas than other biomass-derived activated carbons that do not contain iron. The adsorptive porous activated carbon provides a large surface area while iron oxide facilitates adsorption leading to enhanced performance. Besides, the use of the plant will promote its cultivation leading to consolidated food security as the tubers will be used as food.

This study was aimed at investigating the sorption performance of sweet potato leaf-derived activated carbon on the removal of hydrogen sulphide from biogas.

2. Materials and Methods

2.1. Adsorbent Preparation. Sweet potato leaves were dried using an oven at 100°C, then powdered, sieved, and carbonized in a furnace at 600, 700, and 800°C for 1 h under a constant flow of nitrogen gas to create an inert atmosphere. Carbonization was followed by activation with potassium hydroxide. To activate carbon produced a fixed mass of carbon was mixed with a different mass of KOH in 50 ml of distilled water each time to obtain 1 : 1, 1 : 2, and 1 : 4 KOH : C ratios. A magnetic stirrer was then used to stir the mixture at 80°C for half an hour. The obtained homogeneous mixture was put in an oven to dry at 100°C before being put in a tube

furnace to be activated at 800°C for 1 h under inert condition. Both carbonization and activation were performed at a heating rate of 10°C/min. Activation was followed by washing with 50 ml of dilute HCl and distilled water until neutral pH was obtained; then, the samples were dried for 12 h using an oven at 100°C. After drying, samples were stored for the H$_2$S removal test. The samples obtained were carbonized (C600, C700, and C800), and from each carbonized sample, three activated samples with ratios of 1 : 1, 1 : 2, and 1 : 4 KOH : C were obtained. These are AC600, AC700, and AC800 for each carbonized sample to make a total of nine samples.

2.2. Characterization. Carbonized, activated fresh, and activated spent samples were characterized by BET analysis using Automated gas sorption Quanta chrome porosimeter-Nova 4200 Win © 1994-2013, VII.03 (Boynton Beach Florida, 33426, United States) with nitrogen adsorption-desorption isotherm to measure pore structural properties. Elemental analysis was done using Energy Dispersive X-ray Fluorescence (EDXRF) (Applied Rigaku Technologies, Inc., Austin, TX, 78717, USA) and CHNS analyzer (Hunan Sundy Science and Technology Co., Ltd., China). The surface morphology of the samples was analyzed by Zeiss Ultra Plus Field Emission Scanning Electron Microscopy (FE SEM) (Biocompare South San Francisco, CA, 84080, USA). The functional groups available in the sample surface were studied by Fourier-transform infrared (FTIR) spectroscopy with BRUKER OPAS-FTIR (Mundelein, Illinois 60060, USA).

2.3. Adsorption Test. H$_2$S adsorption experiments were done at the household biogas plant. The setup of the experiment is shown in Figure 1. The valve was used to obtain the desired flow rate (FR) whereby biogas flowed through an inlet of a gas flow rate meter and through the outlet where the bed reactor tube with sample activated carbon supported by cotton wool was connected. The bed reactor tube was connected to the biogas analyzer, which is analyzing the biogas components. Before connecting the bed reactor tube with the sample, the biogas itself was analyzed to record the initial concentration, especially the concentration of H$_2$S.

Removal efficiency (RE) was calculated using equation (1):

$$RE = \frac{C_0 - C}{C_0} \times 100\%, \tag{1}$$

where C_0 and C are the initial and final concentrations of H$_2$S, respectively. Sorption capacity (SC) was calculated using equation (2) [19]:

$$SC = WHSV \times \frac{M}{V_{mol}} \left[\int_0^t (C_0 - C) dt \right], \tag{2}$$

where GHSV is gas hourly space velocity in Lh^{-1} g^{-1}, M is the molar mass of sulphur, V_{mol} is the molar volume of gas in dm^{3}mol, and t is a breakthrough time (BT) in hours at which H$_2$S concentration drops to half of the initial concentration.
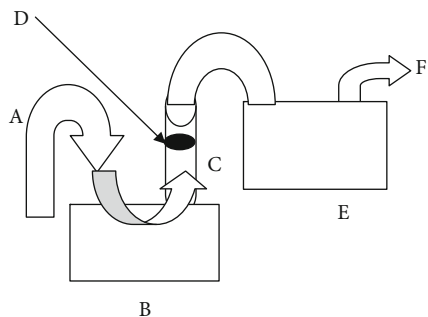
A Gas inlet
C Bed reactor tube
E Biogas analyzer
B Gas flow meter
D Sample supported by cotton wool
F Gas outlet

FIGURE 1: Schematic diagram of the adsorption experiment.

TABLE 1: Composition of biogas.

Constituents	Biogas digester 1	Biogas digester 2
CH_4	66-68%	60-72%
CO_2	35-37%	30-41%
H_2S	500-592 ppm	800-1292 ppm
NH_3	10-18 ppm	17-24 ppm

TABLE 2: XRF analysis of SpLAC.

Minerals	Na_2O	MgO	Al_2O_3	SiO_2	P_2O_5	Fe_2O_3
Conc. (ppm)	5800	34500	5900	34900	24400	5000

2.4. Regeneration of the Sample.

Spent AC is usually regenerated and being reused to avoid disposal costs. The saturated sample was regenerated through a thermal process under the flow of nitrogen gas in the furnace at 220°C for 30 min. After regeneration, the samples were inserted into the bed reactor tube and being tested for adsorption. This method was also used in [25] whereby spent activated carbon was heated in a tube furnace in the presence of inert gas at 220°C for 30 min. The inert gas was purposely used to prevent the burning of activated carbon.

3. Results and Discussion

3.1. Composition of Biogas.

The plant is having two digesters, digester 1 and digester 2, producing biogas composed of methane, carbon dioxide, ammonia, and hydrogen sulphide as shown in Table 1, whereby the quantity of constituents depends on the feedstock used in a particular day. The changes in concentration of H_2S were also examined whereby monitoring showed minimal changes in the initial concentration of H_2S within one hour. That mean nearly constant initial H_2S concentration during sample testing was used.

3.2. Sample Characterization.

XRF analysis for the fresh activated sample prepared at T_c of 800°C and KOH : C of 1 : 1 showed the presence of iron as shown in Table 2, which is

TABLE 3: CHNS analysis of SpLAC.

Elements	C	N	H	S
Wt%	56.25	1.53	2.00	0.00

TABLE 4: Textural properties of activated fresh and activated spent samples.

Sample	BET surface area (m^2/g)	Pore volume (cm^3/g)	Pore diameter (Å)	References
C	637	0.57	30.30	This study
Fresh SpLAC	1220	0.73	30.80	This study
Spent SpLAC	1096	0.67	30.40	This study
Fresh CSAC	726.20	0.40	20.50	[26]
Spent CSAC	607.40	0.30	20.00	[26]

expected to influence the adsorption of hydrogen sulphide through an oxidation reaction.

Carbon was exposed by CHNS analysis, as shown in Table 3.

The surface area is among the substantial characteristics of activated carbon, which has a significant impact on its adsorption efficiency. The surface area depends on the type of pores available. Adsorbent pores are categorized into three classes according to IUPAC: micropores (size < 2 nm), mesopores (2-50 nm), and macrospores (>50 nm). Microspores available and surface area are vastly responsible for the adsorption capacity of activated carbon. Textural parameters, pore diameter, BET surface area, pore volume, micropore area, and mesopore area of the carbonized sample with a carbonization temperature T_c of 800°C and fresh sweet potato leaf-derived activated carbon (SpLAC) with T_c of 800°C and KOH : C of 1 : 1 as well as spent SpLAC which undergone the H_2S sorption are shown in Table 4. This result shows that SpLAC has a higher surface area than the carbonized (C) sample. Activation leads to an increase in surface area and pore volume. Apparently, adsorption process leads to decreased surface area and pore volume. Similar results have been reported for coconut shell activated carbon (CSAC) by [26] as shown in Table 4, whereby fresh CSAC has been found to have a higher surface than the spent CSAC. Therefore, activation process enhances high porosity of the produced activated carbon, resulting in a higher ability to remove H_2S through adsorption.

Figure 2(a) displays N_2 adsorption-desorption isotherms for two samples, fresh and spent SpLAC, and Figure 2(b) displays pore size distribution, calculated by the method known as BJH. As is seen, the fresh activated carbon has a higher N_2 adsorption capacity. The volume of N_2 adsorbed by fresh activated carbon is higher than that adsorbed by a spent sample; thus, the fresh sample exhibits the highest surface area and pore volume (Table 4). Furthermore, SpLAC produced seems to be typical mesoporous carbon by having more pores distributed between 3 and 30 nm as shown in Figure 2(b)
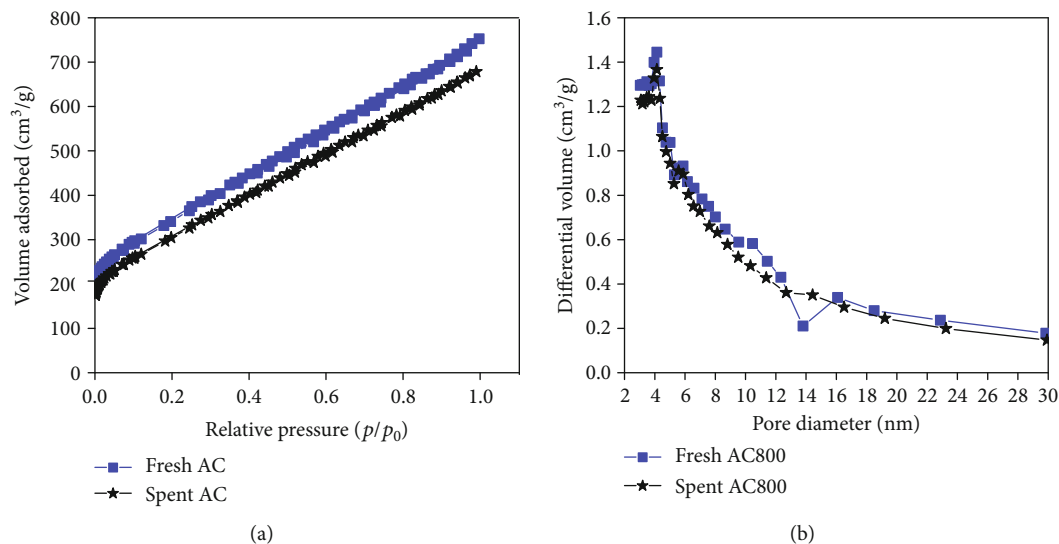
FIGURE 2: (a) Adsorption-desorption isotherms of the activated carbon. (b) Pore size distribution.

TABLE 5: Summary of the results for non-activated and AC sweet potato leaves.

Sample	BT min	RE %	SC (g/100 g)	Micropore area (m^2/g)	Mesopore area (m^2/g)
C800 1:1	30	58	0.90	157	480
AC800 1:1	170	95	3.70	597	623
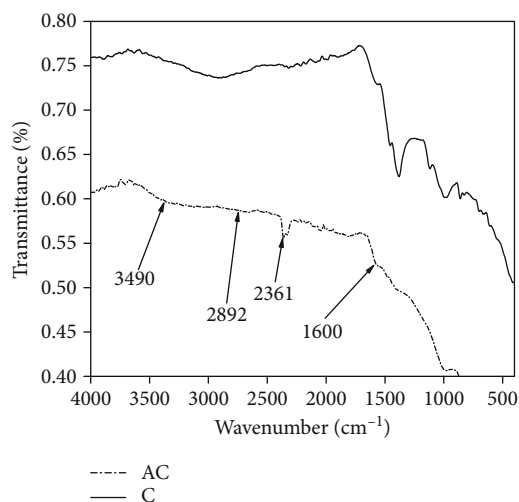
FIGURE 3: FTIR spectrum of carbonized and activated samples.

which indicates that fresh activated sample exhibits higher differential volume than spent activated sample; this is in accordance with their surface area. Similar outcomes may be observed in [27], whereby the AC which was prepared from tomato waste had pores ranging from 4-95 nm showing that the material was mesoporous AC. However, in our case, as it is indicated in Table 5, the BET surface area is contrib-

uted by both the mesopore and micropore areas. Therefore, SpLAC is a promising source of mesopores adsorbent with a certain amount of micropores. We suggest micropores would be more pronounced at a higher KOH:C ratio than 1:1 that has been used as a maximum ratio in this study.

The infrared spectra of carbonized and activated samples are presented in Figure 3. As shown in the figure, the activated sample possesses lower transmittance than the carbonized sample showing that AC has higher absorbance than the carbonized sample. The widespread band around 3490 cm^{-1} indicates O-H stretching; the band around 2892 cm^{-1} is associated with C-H stretching vibration; and the band at 2361 cm^{-1} is probably depicting the alkyne group stretching [28]. The signal around 1600 cm^{-1} is related to aromatic C=C stretching.

The SEM analysis was engaged to study the surface morphology of freshly prepared and spent AC as shown in Figure 4. Both samples were prepared at 1:1 KOH:C ratio which is the highest ratio in this study. Considerable differences may be observed between freshly prepared and spent AC. The micrographs indicate that there are rough surfaces with pores contained on the surface of fresh AC (Figures 4(a) and 4(c)) which were then filled after the adsorption process (Figures 4(b) and 4(d)). This difference might be caused by adsorption of H_2S on the pores of AC which accords well with higher surface area and pore size of fresh SpLAC as presented in Table 4. The mesopores and micropores were created in AC as a result of KOH evaporation during the activation step.

3.3. H_2S Removal by the SpLAC Samples.
Performances of adsorbent samples are shown using a graph of H_2S concentration after sorption and RE against sorbent working time; the effect of different factors is analyzed.

3.3.1. Effect of Carbonization Temperature.
Sweet potato leaf-derived carbon was carbonized at different temperatures, between 600 and 800°C. Effect of carbonization temperature
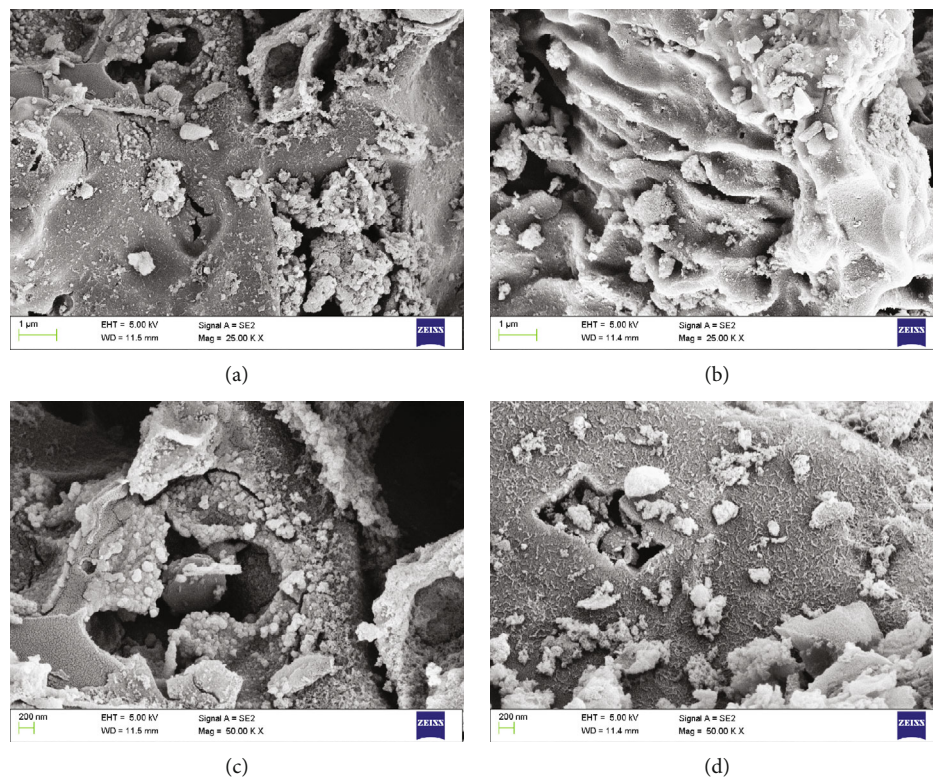
(a)

(b)

(c)

(d)

FIGURE 4: SEM images of the SpLAC sample at low magnification (25.00 KX) and high magnification (50.00 KX). (a, c) Fresh AC and (b, d) spent AC samples.
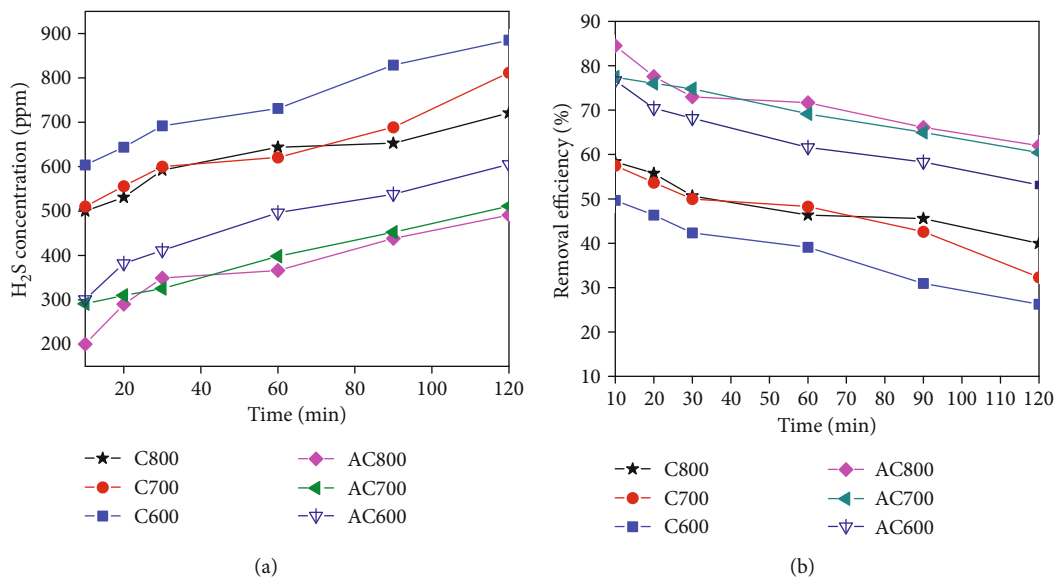

(a)

(b)

FIGURE 5: Effect of carbonization temperature on the samples' adsorption performance: (a) H_2S concentration after sorption; (b) removal efficiency. Test conditions: $m = 0.20$ g, FR $= 0.03$ m^3/h, KOH : C 1 : 1, $C_0 = 1200 - 1290$ ppm.

on hydrogen sulphide removal by samples was considered; the H_2S concentration after sorption was monitored; the readings were taken every 10 min during the test up to approaching sample saturation. Results are displayed both for carbonized samples (C800) and activated samples (AC800) in Figure 5.

Adsorption capacity increases with the increase in carbonization temperature. The sample which was carbonized at high temperature has been found to have higher adsorption capacity, and the sample with lower carbonization temperature has been found to have lower adsorption capacity for both C and AC. The adsorption capacity of activated
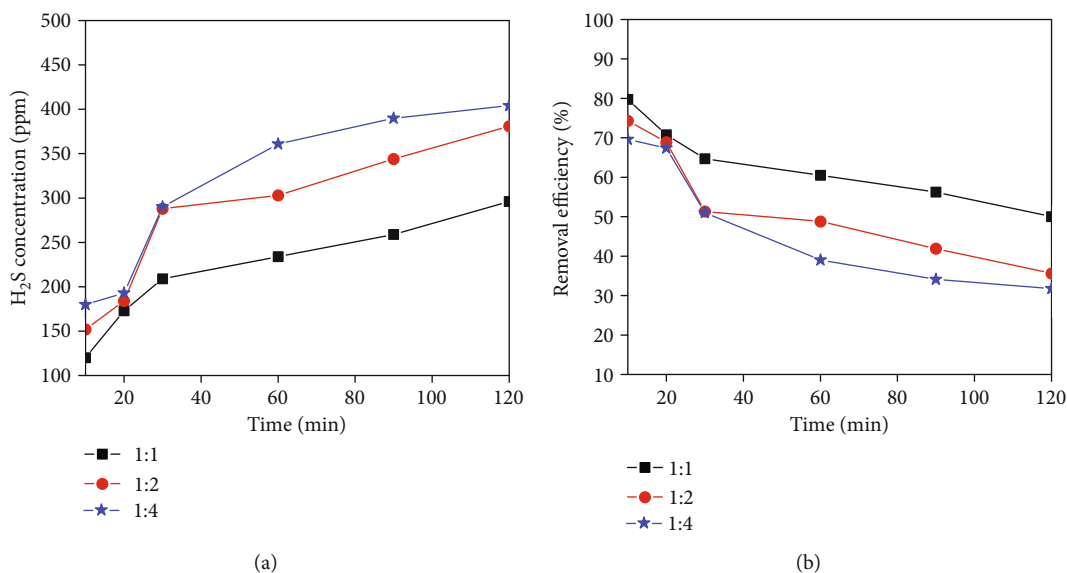
(a)

(b)

FIGURE 6: Effect of the KOH : C ratio on the samples' adsorption performance: (a) H_2S concentration after sorption; (b) removal efficiency. Test conditions: T_c = 800°C, m = 0.3 g, FR = 0.02 m^3/h, C_0 = 592 ppm.
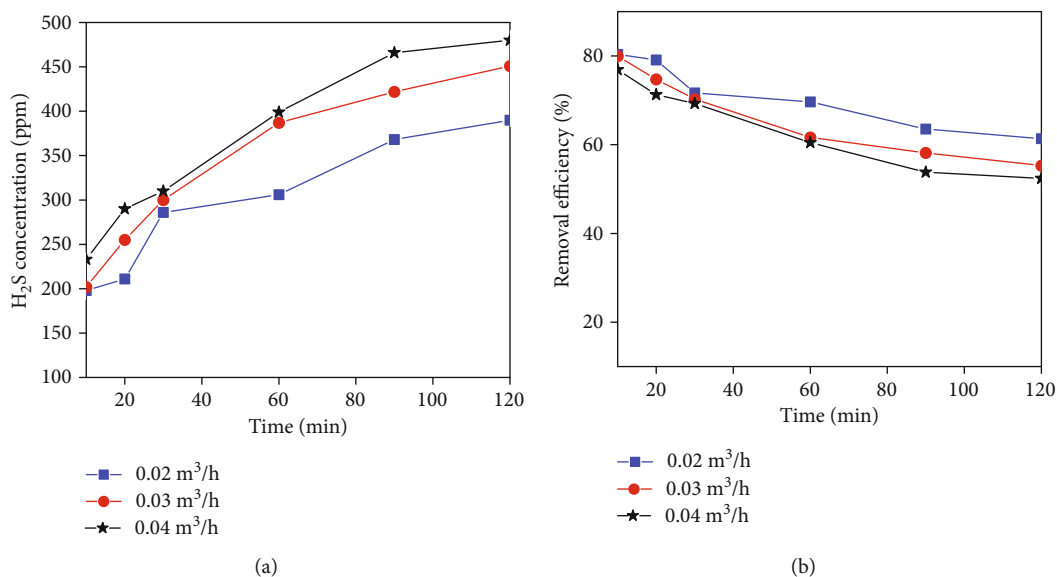

(a)

(b)

FIGURE 7: Effect of biogas flow rate on the samples' adsorption performance: (a) H_2S concentration after sorption; (b) removal efficiency. Test conditions: T_c = 800°C, m = 0.3 g, KOH : C 1 : 1, C_0 = 1009 ppm.

carbon could be profoundly affected by carbonization temperature, which creates initial porosity in the char. The higher the carbonization temperature, the higher the production of micropores hence the production of carbon with high porosity. Adsorption capacity increases with an increase in carbonization temperature; however, activated samples have higher RE of carbonized samples, and this shows the significance of the activation process in the development of micropores essential for adsorption. These results are similar to that of [29] whereby alkali activation works best at a carbonization temperature between 500 and 900°C, and surface area increases concurrently. However, it will decrease at a higher temperature from 800°C to 900°C since at temperatures above 800°C, pores combine to produce mesopores.

3.3.2. Effect of Activation Ratio, KOH : C. The type of the pores to be produced depends on different activation conditions whereby activation ratio is very potential for micropore production when chemical activation is used [30]. Figure 6 displays the effect of the KOH : C ratio on the removal efficiency of SpLAC, whereby three activated carbon samples with different activation ratios were studied. According to results, removal efficiency increases with an increase in activation ratio.

After initial pores have been developed through carbonization, activation enhances further development of pores and produces an ordering of the structure to come up with highly porous activated carbon for improved performance on the adsorption process. Production of micropores increases with
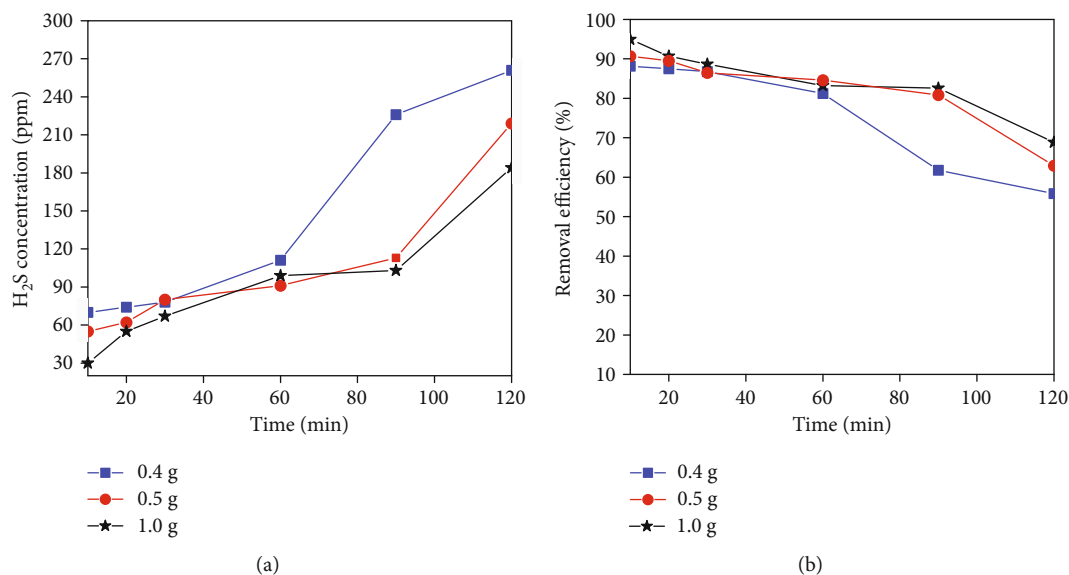
FIGURE 8: Effect of adsorbent mass on the samples' adsorption performance: (a) H_2S concentration after sorption; (b) removal efficiency. Test conditions: T_c = 800°C, FR = 0.02 m³/h, KOH : C ratio 1 : 1, C_0 = 591 ppm.
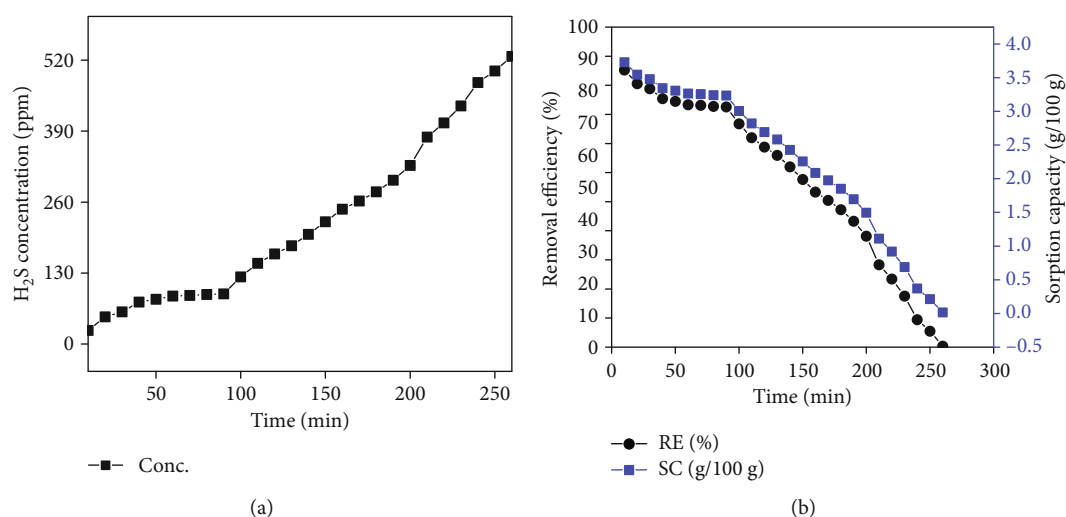

FIGURE 9: (a) H_2S concentration after sorption; (b) removal efficiency and sorption capacity. Test conditions: T_c = 800°C, FR = 0.02 m³/h, m = 1.0 g, KOH : C 1 : 1, C_0 = 529 ppm.

TABLE 6: Comparison of the SpLAC with other materials.

Adsorbent	RE (%)	SC (g, S/100 g, sorbent)	References
Volcanic ash	96	1.00	[19]
Coconut shell AC		2.03	[26]
Zeolite		13.30 -25.20	[33]
Maize cob waste AC		1.60	[16]
SpLAC	95	3.70	This study
Laterite	91.67		[34]

an increase in activation ratio. However, when the amount of activation agent is very high, the yield of activated carbon is decreased, as it has been reported in [31]. According to our study, as it is shown in the graph, the activated carbon with the highest ratio has the highest removal efficiency. There-

fore, it seems that AC with 1 : 1 KOH : C has a higher amount of micropores than others.

3.3.3. Effect of Biogas Flow Rate. Gas flow rate is a potential factor to consider during the adsorption experiment as it is among the factors that facilitate the overall process to come up with efficient adsorption. Figure 7 shows the effect of flow rate on the performance of SpLAC.

It has been found that the RE of activated carbon is high at the lowest flow rate of biogas and low at the highest flow rate of biogas. That is apparently due to the reason that flow rate determines contact time between H_2S and sorbent material. At lower flow rate, the contact time between H_2S and adsorbent is increased hence increasing the chance of all H_2S molecules to be adsorbed from a gas stream until it
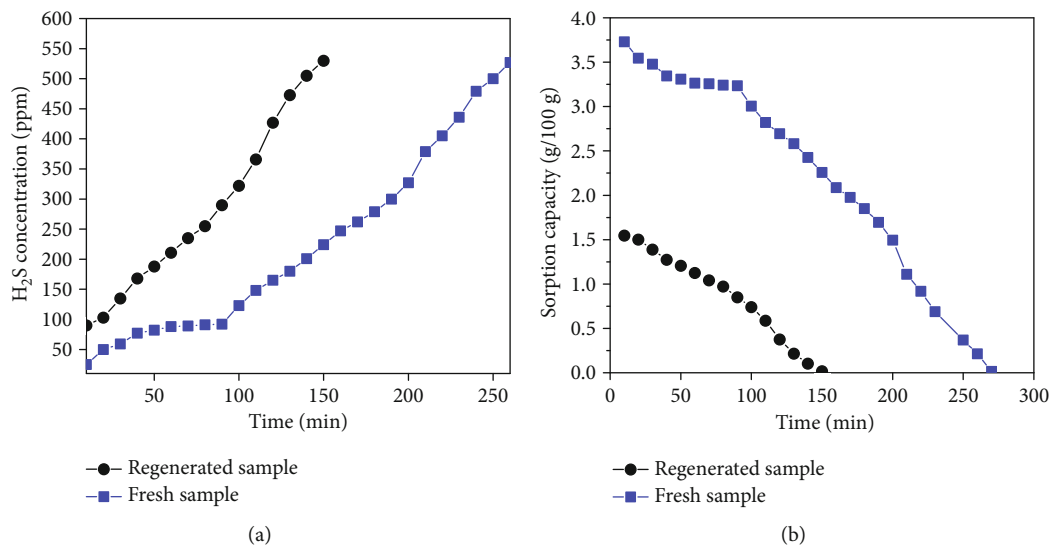
(a)

(b)

Figure 10: Comparison between the fresh sample and regenerated sample: (a) H_2S concentration after sorption by regenerated sample; (b) sorption capacity. Test conditions: $T_c = 800°C$, FR = 0.02 m^3/h, KOH : C 1 : 1, $m = 1.0$ g, $C_0 = 535$ ppm.

reaches a saturation point. Similar phenomena may be observed in [4]. In that study, water hyacinth AC was used to remove H_2S and NH_3 from biogas whereby the lowest flow rate of biogas showed the best results. In addition to that, Oldoinyo Lengai volcanic ashes showed similar outcomes whereby at the lowest biogas flow rate, the samples had the highest removal efficiency.

3.3.4. Effect of Adsorbent Mass. Activation of carbon enhances the development of microspores leading to a large surface area for adsorption. The likelihood of H_2S to contact with adsorption sites on activated carbon surface increases with the increase in the amount of adsorbent. Figure 8 displays the effect of adsorbent mass on the performance of SpLAC. As it is shown in the figure, the RE is increasing with an increase in sorbent mass.

These results could be influenced by a higher amount of activated carbon that enhances larger contact surface area for H_2S to be held into the pores of adsorbent hence higher RE. Similar outcomes may be observed in the studies [4, 19] where the sorption performance of adsorbents increased with an increase of sorbent mass.

3.3.5. Sorption Capacity. Sorption capacity in a gram of sulphur per 100 g of sorbent for both carbonized and activated samples was calculated using equation (2) as portrayed in [19]. Breakthrough time for both carbonized and activated samples is shown in Table 5 together with textural parameters. As is seen, the larger are the pore volume and surface area, the higher are the BT and sorption performance. Figure 9 depicts the SC and RE of the best sample calculated for intervals of 10 min of sorbent working time up to the saturation limit.

Sorption capacity of the adsorbent was decreasing in the same way as removal efficiency with an increase in sorbent working time. The trend is probably determined by saturation of material which is occurring concurrently with sorbent

working time, therefore, decreasing the adsorption process. When the saturation point is reached, both RE and SC are zero showing that initial and final concentrations of H_2S are equal.

Carbon-based sorbents have several mechanisms through which H_2S could be adsorbed. Activated carbon produced with KOH activation is motivated by the pore structure, chiefly with micropores rather than surface chemistry [32]. H_2S adsorption is based on pore structure favouring physisorption, which occurs between the H_2S molecule and the carbon surface. Activation results in widened spaces between carbon atomic layers, thus increasing the total pore volume influencing physisorption. However, the SpLAC contains iron which can also contribute to adsorption as shown in equation (3).

$$Fe_2O_3 + 3H_2S \longrightarrow Fe_2S_3 + 3H_2O \qquad (3)$$
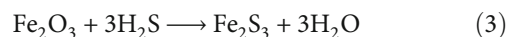
Properties of the SpLAC are compared with other adsorbent materials which were also used to remove H_2S from biogas as shown in Table 6.

As it is shown in Table 6, SpLAC has the highest SC of all except zeolite, which is a rock material; thus, its utilization enhances land degradation.

After saturation was reached, spent AC800 1 : 1 was regenerated and being tested to check its performance in comparison with the freshly prepared AC800 1 : 1. Figure 10 displays the comparison between the fresh sample and the regenerated sample in terms of SC.

As it is shown in Figure 10, the regenerated sample has been found to have lower SC compared with the freshly prepared sample. Sorbent working time for fresh samples is longer than that of the regenerated sample; BTs for fresh and regenerated samples are 170 and 80 min, respectively. The results could be caused by the fact that the regenerated sample is getting saturated faster as compared with the freshly

prepared sample; therefore, regeneration does not reproduce completely the sorption capacity of the sorbent prepared.

4. Conclusions

In this study, the performance of sweet potato's leaf-derived activated carbon for hydrogen sulphide removal from biogas was investigated. According to results, the sample carbonized at 800°C with the activation ratio of 1 : 1 KOH : C showed the highest removal efficiency of about 95% and a sorption capacity of about 3.70 g S/100 g SpLAC. Removal efficiency increased with an increase in carbonization temperature, an increase in sorbent mass, and a decrease in biogas flow rate. The BET analysis showed that activated carbon possessed higher surface area and pore volume as compared with carbonized samples. The elemental analysis, which was performed by XRF, showed the presence of Fe_2O_3, which is significant for the H_2S adsorption process. Generally, novel adsorbent, sweet potato leaf-derived activated carbon is a promising option to replace other adsorbents for hydrogen sulphide removal from biogas.

Data Availability

Data to support this study are available, and correspondence author can be contacted whenever they are needed.

Conflicts of Interest

The authors have confirmed no conflict of interest regarding the publication of this paper.

Acknowledgments

References

[1] N. H. Florin and A. T. Harris, "Enhanced hydrogen production from biomass with in situ carbon dioxide capture using calcium oxide sorbents," *Chemical Engineering Science*, vol. 63, no. 2, pp. 287–316, 2008.

[2] J. Niesner, D. Jecha, and P. Stehlík, "Biogas upgrading technologies: state of art review in European region," *Chemical Engineering Transactions*, vol. 35, pp. 517–522, 2013.

[3] N. Zulkefli, M. Masdar, J. Jahim, and E. Harianto, "Overview of H_2S removal technologies from biogas production," *International Journal of Applied Engineering Research*, vol. 11, pp. 10060–10066, 2016.

[4] E. Makauki, C. K. King'ondu, and T. E. Kibona, "Hydrogen sulfide and ammonia removal from biogas using water hyacinth-derived carbon nanomaterials," *African Journal of Environmental Science and Technology*, vol. 11, no. 7, pp. 375–383, 2017.

[5] S. Heubeck and R. Craggs, "Biogas recovery from a temperate climate covered anaerobic pond," *Water Science and Technology*, vol. 61, no. 4, pp. 1019–1026, 2010.

[6] S. Peiffer and W. Gade, "Reactivity of ferric oxides toward H_2S at low pH," *Environmental Science and Technology*, vol. 41, no. 9, pp. 3159–3164, 2007.

[7] J. Kanjanarong, B. S. Giri, D. P. Jaisi et al., "Removal of hydrogen sulfide generated during anaerobic treatment of sulfate-laden wastewater using biochar: evaluation of efficiency and mechanisms," *Bioresource Technology*, vol. 234, pp. 115–121, 2017.

[8] Y.-C. Chung, K.-L. Ho, and C.-P. Tseng, "Two-stage biofilter for effective NH3 removal from waste gases containing high concentrations of H2S," *Journal of the Air & Waste Management Association*, vol. 57, no. 3, pp. 337–347, 2007.

[9] D. Gabriel and M. A. Deshusses, "Retrofitting existing chemical scrubbers to biotrickling filters for H2S emission control," *Proceedings of the National Academy of Sciences*, vol. 100, no. 11, pp. 6308–6312, 2003.

[10] L. Pokorna-Krayzelova, J. Bartacek, D. Vejmelkova et al., "The use of a silicone-based biomembrane for microaerobic H_2S removal from biogas," *Separation and Purification Technology*, vol. 189, pp. 145–152, 2017.

[11] Y. Belmabkhout, G. De Weireld, and A. Sayari, "Amine-bearing mesoporous silica for CO_2 and H_2S removal from natural gas and biogas," *Langmuir*, vol. 25, no. 23, pp. 13275–13278, 2009.

[12] A. Mitomo, T. Sato, N. Kobayashi, S. Hatano, Y. Itaya, and S. Mori, "Adsorption removal of hydrogen sulfide by activated coke produced from wood pellet in the recycle system of biomass," *Journal of Chemical Engineering of Japan*, vol. 36, no. 9, pp. 1050–1056, 2003.

[13] A. Ros, M. Lillo-Ródenas, E. Fuente, M. Montes-Morán, M. Martín, and A. Linares-Solano, "High surface area materials prepared from sewage sludge-based precursors," *Chemosphere*, vol. 65, no. 1, pp. 132–140, 2006.

[14] T. Alfredy, Y. A. C. Jande, and T. Pogrebnaya, "Removal of lead ions from water by capacitive deionization electrode materials derived from chicken feathers," *Journal of Water Reuse and Desalination*, vol. 9, no. 3, pp. 282–291, 2019.

[15] J. Elisadiki, Y. A. C. Jande, R. L. Machunda, and T. E. Kibona, "Porous carbon derived from *Artocarpus heterophyllus* peels for capacitive deionization electrodes," *Carbon*, vol. 147, pp. 582–593, 2019.

[16] E. Surra, M. Costa Nogueira, M. Bernardo, N. Lapa, I. Esteves, and I. Fonseca, "New adsorbents from maize cob wastes and anaerobic digestate for H_2S removal from biogas," *Waste Management*, vol. 94, pp. 136–145, 2019.

[17] K. Ciahotný and V. Kyselová, "Hydrogen sulfide removal from biogas using carbon impregnated with oxidants," *Energy Fuels*, vol. 33, no. 6, pp. 5316–5321, 2019.

[18] S. Sahota, V. K. Vijay, P. M. V. Subbarao et al., "Characterization of leaf waste based biochar for cost effective hydrogen sulphide removal from biogas," *Bioresource Technology*, vol. 250, pp. 635–641, 2018.

[19] I. Kandola, A. Pogrebnoi, and T. Pogrebnaya, "Oldoinyo Lengai volcanic ash for removal of hydrogen sulfide and ammonia from biogas," *Journal of Materials Science and Chemical Engineering*, vol. 6, no. 4, pp. 78–93, 2018.

[20] P. Cosoli, M. Ferrone, S. Pricl, and M. Fermeglia, "Hydrogen sulphide removal from biogas by zeolite adsorption: part I.

GCMC molecular simulations," *Chemical Engineering Journal*, vol. 145, no. 1, pp. 86–92, 2008.

[21] H. Ishida, H. Suzuno, N. Sugiyama, S. Innami, T. Tadokoro, and A. Maekawa, "Nutritive evaluation on chemical components of leaves, stalks and stems of sweet potatoes (*Ipomoea batatas poir*)," *Food Chemistry*, vol. 68, no. 3, pp. 359–367, 2000.

[22] F. Amagloh, R. Atuna, R. McBride, E. Carey, and T. Christides, "Nutrient and total polyphenol contents of dark green leafy vegetables, and estimation of their iron bioaccessibility using the in vitro digestion/Caco-2 cell model," *Food*, vol. 6, no. 7, p. 54, 2017.

[23] X. Wei, Y. Li, and S. Gao, "Biomass-derived interconnected carbon nanoring electrochemical capacitors with high performance in both strongly acidic and alkaline electrolytes," *Journal of Materials Chemistry A*, vol. 5, no. 1, pp. 181–188, 2017.

[24] A. Davydov, K. T. Chuang, and A. R. Sanger, "Mechanism of H_2S oxidation by ferric oxide and hydroxide surfaces," *The Journal of Physical Chemistry B*, vol. 102, no. 24, pp. 4745–4752, 1998.

[25] T. B. Gebreegziabher, S. Wang, and H. Nam, "Adsorption of H_2S, NH_3 and TMA from indoor air using porous corncob activated carbon: isotherm and kinetics study," *Journal of Environmental Chemical Engineering*, vol. 7, no. 4, article 103234, 2019.

[26] H. S. Choo, L. C. Lau, A. R. Mohamed, and K. T. Lee, "Hydrogen sulfide adsorption by alkaline impregnated coconut shell activated carbon," *Journal of Engineering Science and Technology*, vol. 8, pp. 741–753, 2013.

[27] H. Sayğılı and F. Güzel, "High surface area mesoporous activated carbon from tomato processing solid waste by zinc chloride activation: process optimization, characterization and dyes adsorption," *Journal of Cleaner Production*, vol. 113, pp. 995–1004, 2016.

[28] H. Demiral and C. Güngör, "Adsorption of copper(II) from aqueous solutions on activated carbon prepared from grape bagasse," *Journal of Cleaner Production*, vol. 124, pp. 103–113, 2016.

[29] J.'i. Hayashi, A. Kazehaya, K. Muroyama, and A. P. Watkinson, "Preparation of activated carbon from lignin by chemical activation," *Carbon*, vol. 38, no. 13, pp. 1873–1878, 2000.

[30] O. Üner and Y. Bayrak, "The effect of carbonization temperature, carbonization time and impregnation ratio on the properties of activated carbon produced from *Arundo donax*," *Microporous and Mesoporous Materials*, vol. 268, pp. 225–234, 2018.

[31] Y. Sudaryanto, S. Hartono, W. Irawaty, H. Hindarso, and S. Ismadji, "High surface area activated carbon prepared from cassava peel by chemical activation," *Bioresource Technology*, vol. 97, no. 5, pp. 734–739, 2006.

[32] T. Mochizuki, M. Kubota, H. Matsuda, and L. F. D'Elia Camacho, "Adsorption behaviors of ammonia and hydrogen sulfide on activated carbon prepared from petroleum coke by KOH chemical activation," *Fuel Processing Technology*, vol. 144, pp. 164–169, 2016.

[33] L. Sigot, G. Ducom, and P. Germain, "Adsorption of hydrogen sulfide (H_2S) on zeolite (Z): retention mechanism," *Chemical Engineering Journal*, vol. 287, pp. 47–53, 2016.

[34] N. Thanakunpaisit, N. Jantarachat, and U. Onthong, "Removal of hydrogen sulfide from biogas using laterite materials as an adsorbent," *Energy Procedia*, vol. 138, pp. 1134–1139, 2017.